INTERNATIONAL JOURNAL OF MOLECULAR MEDICINE 24: 343-352, 2009

SPANDIDOS PUBLICATIONS

Alteration of lipid fatty acid profile and cationic fluxes in ventricular cardiomyocytes from ω3-depleted rats

SÉBASTIEN PELTIER[1], KARIM LOUCHAMI[2], YING ZHANG[2], LAURENCE PORTOIS[1], MIRJAM HACQUEBARD[1], WILLY J. MALAISSE[2] and YVON A. CARPENTIER[1]

Laboratories of [1]Experimental Surgery, [2]Experimental Hormonology, Université Libre de Bruxelles, B-1070 Brussels, Belgium

Received April 23, 2009; Accepted June 11, 2009

DOI: 10.3892/ijmm_00000238

Abstract. The bolus intravenous injection of a medium-chain triglyceride:fish oil emulsion was recently found to increase within 60 min the cell phospholipid content in long-chain polyunsaturated ω3 fatty acids and, hence, proposed as a potential tool to prevent cardiac arrhythmia in subjects with a decreased dietary intake of such fatty acids. In the present study, ventricular cardiomyocytes from second generation rats depleted in ω3 fatty acids were found to display the same changes in the phospholipid fatty acid pattern as that previously documented in the cardiac muscle and endothelium of such rats, altered ^{86}Rb and ^{45}Ca fluxes with emphasis on a decrease in both K^+ inflow and K^+ content and an increase in both Ca^{2+} inflow and content. The alteration of K^+ inflow could not be attributed to a decrease in ouabain-sensitive Na^+,K^+-ATPase activity as measured in cell homogenates. The cationic alterations were corrected, in part at least, by the prior intravenous injection of the medium-chain triglyceride:fish oil emulsion 60 min before sacrifice of the ω3-depleted rats.

Introduction

Sudden death provoked by cardiac arrhythmia remains the cause of most deaths in industrialized societies. As reviewed by Carpentier and Hacquebard (1), a rapid supply of long-chain polyunsaturated ω3 fatty acids with resulting prompt incorporation of these fatty acids in cell phospholipids may offer the perspective to reduce the risk of cardiac arrhythmia including ventricular fibrillation. In this respect, administration to healthy male subjects of a novel medium-chain triglyceride:fish oil (8:2, w:v) emulsion (MCT:FO), containing 20% lipids (w/v) and injected as a 50 ml intravenous bolus was indeed found to increase within 60 min and for at least 240 min the eicosapentaenoate content of platelet and leukocyte phospholipids (2), without any alteration of hemostatic variables (3). Preclinical investigations conducted in second-generation ω3-depleted rats have also documented, within 60 min after the intravenous injection of the same emulsion (1.0 ml), both changes in the fatty acid pattern of heart phospholipids and triacylglycerols (4) and improvement of post-ischemic cardiac function (5), as well as remodelling of cationic fluxes in aortic rings (6). Moreover, when either normal or diabetic rats were examined 20 h after injection of the same emulsion (1.0 ml), protection of aortic endothelial function against the deleterious effect of oxidized LDL was observed in experiments conducted *ex vivo* (7).

The present study affords information on the perturbation of lipid fatty acid pattern and cationic fluxes in ventricular cardiomyocytes from second-generation ω3-depleted rats and the partial to total correction of such defects in $^{86}Rb^+$ and $^{45}Ca^{2+}$ handling resulting from the prior intravenous injection of the MCT:FO emulsion one hour before sacrifice.

Materials and methods

Animal model. The present study was carried out in accordance with the principles of the Animal Experimentation Ethics Committee of Brussels Free University Medical School (Belgium). Animals were housed in an animal quarter with control of temperature (24˚C), hygrometry (60%) and brightness/darkness cycle (12 h/12 h). Two groups of animals were used for this study. The first group (control animals) was composed of 21 male Wistar rats (16±1 weeks old, 426±13 g body wt.; Iffa Credo, l'Arbresle, France) fed a commercially available chow diet (AO3; SAFE, Villemoisson-sur-Orge, France). The second group of 46 male Wistar rats (20±1 weeks old, 515±13 g body wt.; UMR 1019 INRA, Université d'Auvergne, Clermont-Ferrand, France) was fed a diet deficient in long-chain polyunsaturated ω3 fatty acids (ω3). The animals were issued from two generations of rats fed the ω3-deficient diet (8). The difference between these two diets is described elsewhere (9). Briefly, the control and ω3-depleted diet contained 5% (wt/wt) lipids from soya and sunflower,

Correspondence to: Professor Willy J. Malaisse, Laboratory of Experimental Hormonology, Université Libre de Bruxelles, 808 Route de Lennik, B-1070 Brussels, Belgium
E-mail: malaisse@ulb.ac.be

Key words: ventricular cardiomyocytes, long-chain polyunsaturated ω3 fatty-acid-depleted rats, medium-chain triglyceride:fish oil emulsion

respectively, with the C18:3ω3 ponderal percentage in fatty acids being ~25 times lower in the latter than in the former diet. All animals had *ad libitum* access to food and water.

Lipid emulsions. MCT:FO and MCT:OO lipid emulsions were manufactured respectively by Grifols (Barcelona, Spain) and B. Braun Melsungen AG (Melsungen, Germany). MCT:FO contained 80% medium chain-triacylglycerols and 20% fish oil with 0.4% (w/v) α-tocopherol. In control MCT:OO emulsion, fish oil was replaced by triolein (10).

Preparation of adult rat ventricular myocytes. The animals were anesthetized by intra-peritoneal injection of pentobarbital sodium (50 mg.kg^{-1} body wt.). Some ω3-depleted rats were injected via the left saphenous vein 60 min before heart removal with 1.0 ml of either MCT:FO or MCT:OO emulsion. These rats are referred to as ω3D-FO and ω3D-OO rats, as distinct from ω3D-NI rats for the uninjected ω3-depleted animals. A rapid thoracotomy was then realized and the heart was quickly removed and immediately immersed in a large volume of cold (4˚C) Ca^{2+}-free Ringer solution composed of (in mM) NaCl 117, KCl 5.7, $NaHCO_3$ 4.4, KH_2PO_4 1.5, $MgCl_2$ 1.7, D-glucose 11.1, creatine 10.0, taurine 20.0 and HEPES 21.0, adjusted to pH 7.1 with NaOH at room temperature. Rapidly, the hearts were mounted on the cannula of a Langendorff apparatus and perfused retrogradedly at a constant flow of 6 ml.min^{-1} and at 37˚C by the Ca^{2+}-free Ringer solution during 4 min followed by 1 h of perfusion at 4 ml.min^{-1} with the dissociation solution. For this enzymatic dissociation solution, 1.0 mg.ml^{-1} collagenase A (Roche, Mannheim, Germany), 300 μM EGTA and $CaCl_2$ (to obtain a free Ca^{2+} concentration of ~20 μM) were added to the Ca^{2+}-free Ringer solution. The perfusion fluids were continuously oxygenated with 95% O_2 - 5% CO_2. At the end of the dissociation period, the ventricles were separated from atria, chopped finely and agitated gently to dissociate individual cells in the Ca^{2+}-free Ringer solution supplemented with $CaCl_2$ (free Ca^{2+} concentration 20-25 μM) (37˚C, pH 7.1, solution I). The resulting cell suspension was filtered through a mesh with a pore size of 220 μm and the cells were then suspended in the solution I. After an incubation period of 5 min at 37˚C during which the cells were allowed to settle down, the supernatant was discarded and replaced by an appropriate volume of the solution I. Then, the cell suspension was agitated during 10 min at 37˚C and the free Ca^{2+} concentration was progressively increased to attain 320-325 μM at the end of the agitation period. Once again, the cell suspension was then incubated during 5 min at 37˚C without agitation to allow the cells to sediment. The supernatant was then removed and the cells resuspended twice in the Ca^{2+}-free Ringer solution supplemented with fatty acid-free bovine serum albumin (5.0 mg/ml^{-1}) (Sigma, Steinheim, Germany) and $CaCl_2$ to obtain a free Ca^{2+} concentration of ~300 μM (37˚C, pH 7.4). Lastly, the cells were transferred in the Ca^{2+}-free Ringer solution enriched with $CaCl_2$ (free Ca^{2+} concentration 1 mM) and 1% penicillin-streptomycin (37˚C, pH 7.4). The cells were then placed in Petri dishes at 37˚C in a tissue culture incubator with 5% CO_2 until use.

Measurement of phospholipid fatty acid pattern. The lipid fatty acid pattern of freshly isolated ventricular cardiomyocytes obtained from normal rats and ω3-depleted rats was determined by a procedure previously described (11,12).

Measurement of $^{86}Rb^+$ uptake. The method used to measure the net uptake of $^{86}Rb^+$ was previously described (13). Briefly, 90 min after the end of the isolation procedure the myocytes were centrifuged (100 x g, 3 min, 20˚C), the supernatant removed and the cells resuspended in an appropriate volume of a bicarbonate- and HEPES-buffered medium containing (in mM) NaCl 111, HEPES 10, $NaHCO_3$ 24, KCl 5, $MgCl_2$ 1, $CaCl_2$ 1, D-glucose 8.3 and 1.0 mg.ml^{-1} fatty acid-free bovine serum albumin (Sigma). The cell suspension (25 μl) (~50,000 cells) was then placed in polyethylene tubes and, after addition of 25 μl of the bicarbonate- and HEPES-buffered medium containing, when so required, 200 μM ouabain, pre-incubated for 20 min at 37˚C. Then, 50 μl of the bicarbonate and HEPES-buffered medium containing ^{86}RbCl (50 μCi.ml^{-1}) were added to each tube. After 10 or 60 min incubation at 37˚C, the tubes were centrifuged (1,000 x g, 1 min, 4˚C) and a layer (150 μl) of dibutylphthalate was added. The cells were then separated from the incubation medium by centrifugation (1,000 x g, 3 min, 4˚C) and the tubes were cut so that the bottom contained cells and part of the oil layer. The radioactive content was then examined by liquid scintillation.

Measurement of $^{45}Ca^{2+}$ uptake. Cell suspension (25 μl) (~50,000 cells; see above) placed in the polyethylene tubes were mixed with 25 μl of the bicarbonate and HEPES-buffered medium containing $^{45}Ca^{2+}$ (8.2 μCi.ml^{-1}). This medium contained, as required, NaCl 115 mM and KCl 5 mM, NaCl 65 mM and KCl 55 mM, or NaCl 5 mM and KCl 115 mM, so that the final K^+ concentration of the incubation medium amounted to 5, 30 or 60 mM. After 10 or 60 min of incubation at 37˚C, the same procedure as that used for $^{86}Rb^+$ uptake measurement was followed.

Analysis of cationic fluxes. The analysis of data was conducted as described elsewhere (14). It is based on the assumption that the time course for the net uptake of ^{86}Rb or ^{45}Ca (U), as a function of time (t, expressed as min), corresponds to the following equation: $U=U_{max}\ (1-e^{-Kt})$, equation in which U_{max} and K refer, respectively, to the net uptake of the tracer under consideration at isotopic equilibrium and its fractional outflow rate from the cells (expressed as min^{-1}). The fractional outflow rate was calculated from the values for the net uptake of ^{86}Rb and ^{45}Ca at min 60, expressed relative to those recorded within the same experiment(s) at min 10. The U_{max} was then calculated from the fractional outflow rate and the mean absolute values for ^{86}Rb and ^{45}Ca net uptake recorded after 10 or 60 min incubation under the same experimental conditions. The mean values derived from these two estimations (and the deviation from mean values) were then used to assess the cationic inflow-outflow rate at isotopic equilibrium (i.e. U_{max} x K).

Measurement of distribution spaces. For measuring the ^3H_2O and [U-^{14}C]sucrose of L-[1-^{14}C]glucose distribution spaces,

fatty acid pattern of phospholipids (PL) and triglycerides (TG).

Rats	Control		ω3-depleted	
Lipids	PL	TG	PL	TG
C14:0 (%)	0.0±0.0 (7)	0.8±0.2 (7)	0.0±0.0 (8)	1.4±0.2 (8)
C16:0 (%)	9.1±0.2 (7)	20.6±0.6 (7)	9.5±0.1 (8)	21.6±1.9 (8)
C16:1ω7 (%)	0.1±0.0 (7)	0.4±0.2 (7)	0.3±0.0 (8)	1.7±0.4 (8)
C18:0 (%)	17.8±0.2 (7)	8.5±0.6 (7)	21.1±0.4 (8)	4.5±1.2 (8)
C18:1ω9 (%)	2.5±0.2 (7)	10.0±2.7 (7)	3.8±0.1 (8)	23.5±1.9 (8)
C18:2ω6 (%)	26.8±1.5 (7)	33.9±1.3 (7)	31.1±0.9 (8)	39.4±2.6 (8)
C20:0 (%)	0.3±0.0 (7)	0.7±0.3 (7)	0.3±0.0 (8)	1.4±0.3 (8)
C18:3ω3 (%)	0.2±0.0 (7)	1.3±0.2 (7)	0.0±0.0 (8)	0.0±0.0 (8)
C20:1ω9 (%)	0.1±0.0 (7)	0.1±0.1 (7)	0.1±0.0 (8)	0.0±0.0 (8)
C20:2ω6 (%)	0.3±0.0 (7)	0.5±0.2 (7)	0.2±0.0 (8)	0.2±0.1 (8)
C20:3ω6 (%)	0.2±0.0 (7)	0.0±0.0 (7)	0.0±0.0 (8)	0.0±0.0 (8)
C22:0 (%)	0.2±0.0 (7)	0.0±0.0 (7)	0.4±0.0 (8)	0.0±0.0 (8)
C20:4ω6 (%)	21.6±0.6 (7)	8.1±0.9 (7)	30.1±0.5 (8)	0.0±0.0 (8)
C22:1ω9 (%)	0.2±0.0 (7)	0.0±0.0 (7)	0.1±0.0 (8)	0.0±0.0 (8)
C20:5ω3 (%)	0.1±0.0 (7)	0.0±0.0 (7)	0.0±0.0 (8)	0.0±0.0 (8)
C24:0 (%)	0.1±0.0 (7)	0.0±0.0 (7)	0.2±0.0 (1)	0.0±0.0 (8)
C22:4ω6 (%)	0.5±0.0 (7)	0.7±0.2 (7)	1.8±0.1 (8)	1.8±0.5 (8)
C22:5ω3 (%)	2.3±0.1 (7)	2.6±0.5 (7)	0.1±0.0 (8)	0.0±0.0 (8)
C22:6ω3 (%)	17.5±1.0 (7)	10.3±1.4 (7)	0.8±0.1 (8)	0.0±0.0 (8)

25 μl of the bicarbonate- and HEPES-buffered medium containing tracer amounts of ^3H_2O and either [U-^{14}C]sucrose or L-[1-^{14}C]glucose mixed with 2.0 mM of the unlabelled corresponding sugar were added to 25 μl cell suspension. The tubes were then incubated during 5 min at 37˚C and the procedure described above was again followed.

Na^+,K^+-ATPase activity. The assay or Na^+-K^+-ATPase was conducted in 60 μl of cardiomyocyte homogenates, these samples contained 1.22±0.10 μg DNA (n=20), with a mean DNA content of 73.2±12.1 pg DNA/cell (n=20). For such a purpose, frozen cardiomyocytes stored at -80˚C were defrosted and sonicated on ice thrice for 10 sec. After removal of an aliquot part for DNA dosage, the sonicates were centrifuged at 4˚C and 13,000 x g for 30 min, the supernatant being then diluted in a 1:3 ratio with a histidine-HCl buffer (pH 7.2) containing 20 mM histidine, 6 mM $MgCl_2$, 20 mM KCl, 80 mM NaCl and 20 mM NaN_3. Cell homogenate (60 μl) was mixed with 100 μl of a 1.0 mM ATP solution (also prepared in the histidine-HCl buffer) and 40 μl of the same buffer containing, when so required, 12 mM ouabain. After 30 min incubation at 37˚C, the reaction was halted by heating for 10 min at 70˚C. The resulting reaction mixture was stored at -20˚C, and eventually examined for its inorganic phosphate content. In the 1-10 and 10-100 nmol/sample range, the inorganic phosphate standards yielded rectilinear absorbance/concentration relationships.

Presentation of results. All results are expressed as mean values (± SEM) together with the number of individual determinations (n) or degree of freedom (df). The statistical significance of differences between mean values was assessed by use of Student's t-test.

Results

Fatty acid pattern of cardiomyocyte lipids. Phospholipids. In the cardiomyocytes from ω3-depleted rats, the phospholipid fatty acid pattern displayed several anomalies, tightly resembling those previously documented in the heart of comparable rats (4).

First, at variance with the situation found in control animals, no C18:3ω3 and C20:5ω3 was detected in the phospholipids of ω3-depleted rats. The weight percentage of C22:5ω3 and C22:6ω3 was one order of magnitude lower in the latter rats than in control animals (Table I).

The C22:6ω3/C22:5ω3 ratio was also significantly lower ($p<0.02$) in the ω3-depleted rats than in the control animals, suggesting facilitated generation of C22:5ω3 from C22:6ω3 in the former rats (Table II).

Second, the weight percentage of the three major long-chain polyunsaturated ω6 fatty acids in phospholipids (C18:2ω6, C20:4ω6 and C22:4ω6) was, on the contrary, higher ($p<0.03$ or less) in the ω3-depleted rats than in the control animals. Moreover, the mean values for the C20:4ω6/C18:2ω6 and C22:4ω6/C20:4ω6 ratios were also higher in the ω3-depleted rats than in control animals. Such a difference failed to achieve statistical significance ($p<0.08$) in the case of the C20:4ω6/C18:2ω6 ratio, but was highly significant ($p<0.001$) in the case of the C22:4ω6/C20:4ω6 ratio. These findings thus suggest facilitated generation of C20:4ω6 and C22:4ω6 from their respective precursors in the ω3-depleted rats.

Table II. Paired ratio between distinct fatty acids in the phospholipids.

Rats	Control	ω3-depleted
C22:6ω3/C22:5ω3	7.65±0.15 (7)	6.05±0.51 (8)
C20:4ω6/C18:2ω6	0.83±0.07 (7)	0.98±0.04 (8)
C22:4ω6/C20:4ω6 (x10^3)	23.9±2.1 (7)	59.5±2.3 (8)
C16:1ω7/C16:0 (x10^3)	12.9±1.1 (7)	32.3±1.2 (8)
C18:1ω9/C18:0	0.139±0.011 (7)	0.185±0.006 (8)
C18:0/C16:0	1.97±0.04 (7)	2.23±0.06 (8)
C20:0/C18:0 (x10^3)	15.0±0.8 (7)	13.0±0.5 (8)
C22:0/C20:0	0.84±0.03 (7)	1.40±0.04 (8)
C24:0/C22:0	0.53±0.00 (7)	0.44±0.02 (8)
C20:1ω9/C18:1ω9 (x10^3)	33.3±2.3 (7)	29.2±4.1 (6)
C22:1ω9/C20:1ω9	1.81±0.34 (7)	1.58±0.16 (5)

Third, both the phospholipid C16:1ω7/C16:0 and C18:1ω9/C18:0 ratios were higher ($p<0.005$ or less) in ω3-depleted rats than in control animals, suggesting increased activity of Δ9-desaturase.

Fourth, as judged from the C18:0/C16:0 and C22:0/C20:0 ratio, the elongation of the concerned fatty acids was favoured ($p<0.01$ or less) in the ω3-depleted rats. A mirror image prevailed, however, in the case of the C20:0/C18:0 ($p<0.05$) and C24:0/C22:0 ($p<0.005$) ratio.

Last, when considering the pathway leading to the generation of nervonic acid, the C18:1ω9/C18:0 ratio was, as already mentioned, higher ($p<0.005$) in the ω3-depleted rats than in the control animals. However, such was no more the case for the C20:1ω9/C18:1ω9 and C22:1ω9/C20:1ω9 ratios, which, even if ignoring null values found in the ω3-depleted rats, remained lower, albeit not significantly so ($p>0.3$ or more), in the latter rats than in control animals.

Triglycerides. The total fatty acid content of triglycerides, expressed relative to that of phospholipids failed to differ significantly ($p>0.3$) in control rats (56.0±8.4 μg/mg; n=7) and ω3-depleted rats (67.2±8.0 μg/mg; n=8).

However, the fatty acid pattern of triglycerides differed in several respects when comparing ω3-depleted rats to control animals.

First, whilst sizeable amounts of C18:3ω3, C22:5ω3 and C22:6ω3 were present in the control animals, none of these long-chain polyunsaturated ω3 fatty acids was detected in any ω3-depleted rats (Table I).

Second, in sharp contrast to the situation found in phospholipids, the amount of long-chain polyunsaturated ω6 fatty acids in the triglycerides was about thrice lower ($p<0.007$) in ω3-depleted rats (33.6±5.5 μg/10^6 cells; n=8) than in control animals (90.9±17.9 μg/10^6 cells; n=7). As a matter of fact, the mean value for the triglyceride content of each long-chain polyunsaturated ω6 fatty acid (C18:2ω6, C18:3ω6, C20:2ω6, C20:4ω6 and C22:4ω6) was lower in ω3-depleted rats than in control animals (Table III). Such a difference achieved statistical significance for the two most abundant ω6 fatty acids, i.e. C18:2ω6 ($p<0.02$) and C20:4ω6 ($p<0.001$).

Table III. Absolute values (μg/10^6 cells) for the triglyceride content in long-chain polyunsaturated ω6 fatty acids.

Rats	Control	ω3-depleted	P
C18:2ω6	70.73±13.68 (7)	31.81±4.97 (8)	<0.02
C18:3ω6	0.90±0.73 (7)	0.00±0.00 (8)	<0.21
C20:2ω6	1.31±0.59 (7)	0.22±0.18 (8)	<0.09
C20:4ω6	16.26±3.65 (7)	0.00±0.00 (8)	<0.001
C22:4ω6	1.67±0.64 (7)	1.55±0.51 (8)	<0.90
All	90.87±17.92 (7)	33.58±5.46 (8)	<0.007

Nevertheless, the overall efficiency of the metabolism of long-chain polyunsaturated fatty acids, as judged from the C22:4ω6/C18:2ω6 ratio, was higher ($p<0.04$) in ω3-depleted rats (59.9±10.5x10^{-3}; n=6) than in control animals (29.9±2.9x10^{-3}; n=5).

Third, the C16:1ω7/C16:0 ratio whenever not yielding a null value, was almost twice higher ($p<0.006$) in ω3-depleted rats (98.7±5.4x10^{-3}; n=6) than in control animals (56.5±1.3x10^{-3}; n=2). Likewise, even if ignoring both 2 samples from control animals, in which no C18:1ω9 could be detected, and 3 samples from ω3-depleted rats, in which the C18:0 content of triglycerides did not exceed 0.68±0.65 μg/10^6 cells, the C18:1ω9/C18:0 ratio remained twice higher ($p<0.05$) in the ω3-depleted rats (3.86±0.76; n=5) than in the control animals (1.83±0.33; n=5).

Last, as judged from the (C18:0+C18:1ω9)/(C16:0+C16:1ω7) ratio, the elongase activity was not significantly different ($p>0.1$) in the ω3-depleted rats (1.21±0.18; n=8) and control animals (0.83±0.14; n=7).

Diglycerides. Sizeable amounts of diglycerides were found in 5 out of 7 control animals and 7 out of 8 ω3-depleted rats, with overall mean values for the diglyceride/phospholipid fatty acid content of 4.19±1.25 μg/mg (n=7) in the former animals and 5.66±0.89 μg/mg (n=8) in the latter rats.

When present in detectable amounts, the diglyceride content in C22:6ω3 averaged 4.10±0.94 μg/10^6 cells (n=3) in the cardiomyocytes from control animals. This was the sole long-chain polyunsaturated ω3 fatty acids detected in the diglycerides of these animals. No long-chain polyunsaturated ω3 fatty acid was detected in the diglycerides of ω3-depleted rats (Table IV).

Among the long-chain polyunsaturated ω6 fatty acids, only C18:2ω6 and C20:4ω6 were on occasion found in the diglycerides of control rats, with mean respective values of 6.89±2.60 and 3.24±0.55 μg/10^6 cells (n=5 in both cases). Only C18:2ω6 was detected in 7 out 8 ω3-depleted rats with a mean value 2.62±0.46 μg/10^6 cells. The diglyceride total content in long-chain polyunsaturated ω6 fatty acids was thus lower ($p<0.02$) in the ω3-depleted rats than in the control animals (10.13±3.11 μg/10^6 cells; n=5), a situation comparable to that found in triglycerides.

Sizeable amount of C16:0, C18:0 and C18:1ω9 were, on occasion, also found in both control animals and ω3-depleted rats, in which they averaged respectively 3.62±0.23 μg/10^6

Fatty acid pattern of diglycerides (DG) and unesterified fatty acids (UFA).

Rats	Control		ω3-depleted	
Lipids	DG	UFA	DG	UFA
C16:0 (μg/10^6 cells)	3.62±0.23 (5)	2.65±0.41 (7)	2.71±0.43 (7)	4.08±2.60 (3)
C18:0 (μg/10^6 cells)	3.80±0.70 (5)	4.08±0.45 (7)	2.07±0.31 (7)	4.18±2.51 (4)
C18:1ω9 (μg/10^6 cells)	1.71±0.12 (3)	1.53 (1)	1.43±0.39 (4)	1.76±0.12 (3)
C18:2ω6 (μg/10^6 cells)	6.89±0.26 (5)	2.59±0.23 (6)	2.62±0.46 (7)	1.85±0.36 (5)
C20:4ω6 (μg/10^6 cells)	3.24±0.55 (5)	2.20±0.05 (3)	0.84 (1)	N.D.
C22:6ω3 (μg/10^6 cells)	4.10±0.94 (3)	2.69±0.44 (3)	N.D.	N.D.

N.D., never detected.

Table V. Distribution spaces.

Rats	Control	ω3-depleted
^{3}HOH (pl/cell)	18.50±1.95 (21)	19.67±0.95 (115)
[U-^{14}C]sucrose (pl/cell)	7.27±0.83 (21)	
L-[1-^{14}C]glucose (pl/cell)		8.84±0.74 (115)
Intracellular space (pl/cell)	11.23±1.23 (21)	10.83±0.40 (115)
Extracellular space (% ^{3}HOH space)	38.6±2.0 (21)	37.9±1.8 (115)

cells (n=5) and 2.71±0.43 μg/10^6 cells (n=7) in the case of C16:0, 3.80±0.70 μg/10^6 cells (n=5) and 2.07±0.31 μg/10^6 cells (n=7) in the case of C18:0, and 1.71±0.12 μg/10^6 cells (n=3) and 1.43±0.39 μg/10^6 cells (n=4) in the case of C18:1ω9. The values recorded in the ω3-depleted rats for these 3 fatty acids thus only represented 68.9±7.6% (n=18, $p<0.01$) of the corresponding mean values found in control animals (100.0±7.1%; n=18). The mean paired C18:1ω9/C18:0 ratio was higher, albeit not significantly so ($p>0.2$), in ω3-depleted rats (0.656±0.166; n=4) than in control animals (0.393±0.049; n=3).

Unesterified fatty acids. Whether expressed as μg/10^6 cells or relative to the fatty acid content of phospholipids the total amount of unesterified fatty acids found in the cardiomyocytes failed to differ significantly ($p>0.14$ or more) in control animals and ω3-depleted rats, with overall mean values of 8.40±1.88 μg/10^6 cells and 3.96±1.20 μg/mg (n=15 in both cases).

The sole long-chain polyunsaturated ω3 fatty acids found, on occasion, and solely in a few control animals (3 out of 7 animals), was C22:6ω3, which averaged in these 3 control animals 2.69±0.44 μg/10^6 cells (Table IV).

Among the long-chain polyunsaturated ω6 fatty acids, only C18:2ω6 and C20:4ω6 were detected in some control animals, in which they averaged respectively 2.59±0.23 μg/10^6 cells (n=6) and 2.20±0.05 μg/10^6 cells (n=3). In the ω3-depleted rats, only C18:2ω6 was present, averaging 1.85±0.36 μg/10^6 cells (n=5). The total amount of long-chain polyunsaturated ω6 fatty acids was thus twice higher ($p<0.02$) in control animals (3.69±0.49 μg/10^6 cells; n=6) than in ω3-depleted rats. This finding is comparable to those made in triglycerides and diglycerides.

The two other sole unesterified fatty acids found in the cardiomyocytes of most control animals were C16:0 (2.65±0.41 μg/10^6 cells; n=7) and C18:0 (4.08±0.45 μg/10^6 cells; n=7). The corresponding values in ω3-depleted rats were 4.08±2.60 μg/10^6 cells (n=3) for C16:0 and 4.18±2.51 μg/10^6 cells (n=4) for C18:0. The C18:0/C16:0 ratio averaged 1.63±0.12 (n=7) and 1.61±0.35 (n=3) in the control animals and ω3-depleted rats, respectively.

Cell volume and extracellular space. As shown in Table V, after 5 min incubation at 37˚C, the ^{3}HOH distribution space and that of the extracellular markers ([U-^{14}C]sucrose or L-[1-^{14}C]glucose) were not significantly different in control and ω3D rats. Such was also the case for the intracellular space, taken as the difference between the ^{3}HOH and extracellular spaces. In the light of these findings, no correction was made for extracellular contamination in the further analysis of the measurements for ^{45}Ca and ^{86}Rb net uptake. Nevertheless, it should be kept in mind that such an extracellular contamination was not negligible. For instance, when considering the basal results for ^{86}Rb uptake recorded after 60 min incubation of cells from control rats, the extracellular and intracellular amounts of the radioactive tracer, expressed as K^+ equivalent, yielded respective values 36.4±4.2 and 508.8±35.1 fmol/cell, the latter value corresponding to an apparent intracellular K^+ concentration of 45.3±3.1 mM (d.f.=60). Likewise, the basal results for ^{45}Ca uptake after 60 min incubation of cells from control rats yielded respective extracellular and intracellular amounts of 7.3±0.8 and 24.2±3.2 fmol/cell, the latter value corresponding to an apparent intracellular Ca^{2+} concentration of 2.2±0.3 mM (d.f.=53).

^{86}Rb net uptake. Under the present experimental conditions, preincubation for 20 min at 37˚C in the presence of 0.1 mM ouabain followed by 10-60 min incubation at 37˚C in the presence of 0.05 mM ouabain failed to cause marked changes in ^{86}Rb net uptake (Table VI). For instance, after 60 min incubation the net uptake of ^{86}Rb by cells from control rats and ω3D rats injected with the MCT:FO emulsion averaged

Table VI. ^{86}Rb uptake.

Rats		Control	ω3D-NI	ω3D-OO	ω3D-FO
^{86}Rb net uptake (fmol/cell)					
- Total	min 10	300.1±17.2 (42)	97.4±7.5 (34)	92.5±4.6 (41)	135.5±9.7 (43)
	min 60	545.2±24.9 (41)	193.6±90 (34)	178.6±9.4 (38)	259.3±12.0 (43)
- Ouabain-resistant	min 10	283.8±14.4 (42)	127.6±10.1 (34)	93.1±5.1 (37)	129.4±6.0 (43)
	min 60	491.9±21.2 (42)	189.1±8.9 (34)	176.7±8.1 (40)	237.2±13.0 (43)
^{86}Rb net uptake (% of min 10)					
- Total	min 10	100.0±4.4 (42)	100.0±5.1 (34)	100.0±4.2 (41)	100.0±3.9 (43)
	min 60	177.0±4.4 (41)	202.3±5.1 (34)	183.2±4.1 (38)	198.6±3.9 (43)
^{86}Rb fractional outflow rate (min^{-1})					
- Total		0.082	0.067	0.078	0.068
Isotopic equilibrium data for total uptake					
- K^+ cell content (fmol/cell)		542.7±6.5	198.2±1.1	175.5±4.7	269.2±5.4
- K^+ inflow-outflow (fmol/min per cell)		44.5±0.5	13.3 ± 0.1	13.7±0.4	18.3±0.4

Table VII. ^{45}Ca uptake.

Rats	Control	ω3D-NI	ω3D-FO
^{45}Ca net uptake (fmol/cell at min 10)			
- At 5 mM K^+	14.12±1.60 (27)	18.03±1.66 (31)	9.90±1.02 (32)
- At 30 mM K^+	22.36±1.78 (26)	27.39±2.10 (32)	21.29±1.22 (32)
- AT 60 mM K^+	25.47±2.27 (32)	38.49±2.28 (32)	27.68±0.89 (33)
^{45}Ca net uptake at 60 min (% of min 10)			
- At 5 mM K^+	192.9±7.6 (34)	230.0±7.9 (32)	268.1±12.1 (33)
- At 60 mM K^+	181.9±6.9 (32)	170.9±4.7 (32)	177.4±2.4 (33)
^{45}Ca fractional outflow rate (min^{-1})			
- at 5 mM K^+	0.072	0.054	0.042
- At 60 mM K^+	0.079	0.087	0.082
Equilibrium Ca^{2+} cell content (fmol/cell)			
- At 5 mM K^+	29.70±2.19	42.96±0.25	33.63±4.77
- At 60 mM K^+	46.86±0.22	65.29±0.96	49.71±0.26
Equilibrium Ca^{2+} inflow-outflow (fmol/min per cell)			
- At 5 mM K^+	2.14±0.16	2.32±0.01	1.41±0.20
- At 60 mM K^+	3.70±0.02	5.68±0.08	4.08±0.02

90.9±3.2% (n=85; p<0.006) of the mean corresponding values found after preincubation and incubation in the absence of ouabain. In the cells obtained from ω3D rats, either uninjected or injected with the MCT:OO emulsion 60 min before sacrifice, such a percentage averaged 98.3±3.2% (n=74; p>0.6). When taking into account extracellular contamination, the results recorded in the control and ω3D-FO rats indicated that, in these animals, ouabain decreased the K^+ cell content after 60 min incubation by no more than 10.4±0.1% (n=2).

Whether after 10 or 60 min incubation and whether in the presence or absence of ouabain, the net uptake of $^{86}Rb^+$ was severely decreased (p<0.001) in either the ω3D-NI or ω3D-OO rats, averaging respectively 37.8±1.3% (n=136) and 33.1±0.8% (n=156) of the results found, under the same experimental conditions in control animals (100.0±2.5%; n=167). In the ω3D-FO rats, however, the net uptake of ^{86}Rb represented 46.6±1.3% (n=172) of the control values and, as such, was significantly higher (p<0.001) than that recorded in either ω3D-NI or ω3D-OO rats.

Only minor differences were observed in the time course for ^{86}Rb net uptake in the four groups of rats (Table VI). The results recorded after 60 min incubation, when expressed relative to those recorded in the same experiments after only

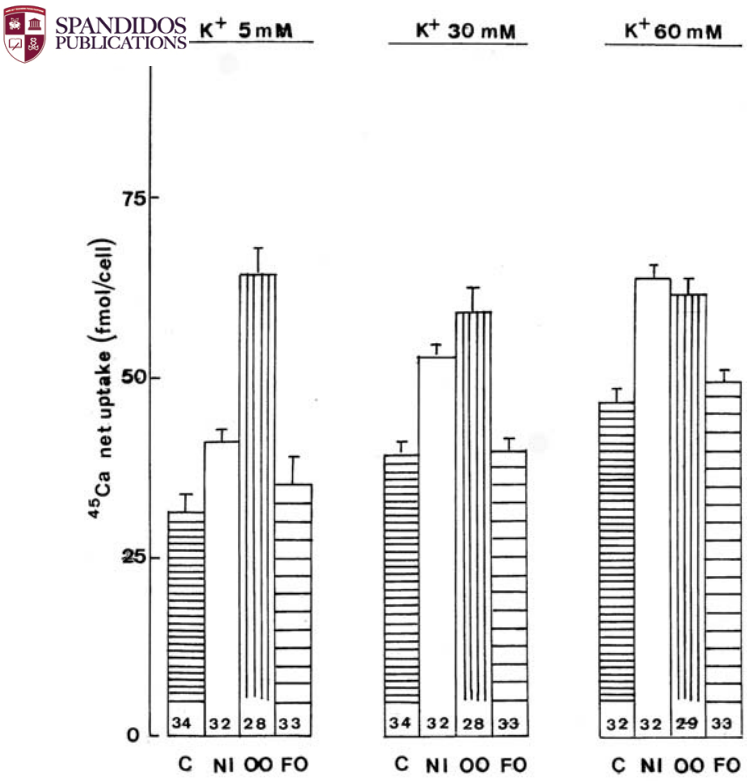

Figure 1. Mean values (± SEM) for the net uptake of ^{45}Ca by cardiomyocytes from control (C), ω3D-NI (NI), ω3D-OO (OO) and ω3D-FO (FO) rats incubated for 60 min at increasing extracellular K^+ concentrations. The number of determinations is shown at the bottom of each column.

10 min incubation, averaged in the ω3-depleted rats 194.6±2.6% (n=115), as distinct (p<0.001) from only 177.0±4.4% (n=41) in the control animals. In this respect, no significant difference (p>0.5) was observed between ω3D-NI and ω3D-FO rats. The difference between control rats and either ω3D-NI or ω3D-FO rats remained significant (p<0.01) when the SEM on both the 10 min reference data (ranging between 3.9 and 5.1%) and the 60 min data (see above) were taken into account. Even the most pronounced difference in the time course for ^{86}Rb net uptake, i.e. that observed between control animals and ω3D-NI rats, only resulted in a modest decrease of the estimated ^{86}Rb fractional outflow rate from 0.082 min^{-1} in the former animals to 0.067 min^{-1} in the latter rats.

The just-mentioned modest difference in the ^{86}Rb fractional outflow rate was obviously not sufficient to mask the marked changes in both the cell K^+ content at isotopic equilibrium and corresponding K^+ outflow-inflow rate (Table VI). Taking into account the ^{86}Rb fractional outflow rate and the absolute values for ^{86}Rb net uptake, as measured after 10 and 60 min incubation, the equilibrium cell K^+ content averaged 543±6 fmol/cell in control rats, as distinct from 198±1 and 175±5 fmol/cell in ω3D-NI and ω3D-OO rats and 269±5 fmol/cells in ω3D-FO rats. Likewise, the estimated inflow-outflow rate of K^+ amounted to 44.5±0.5 fmol/min per cell in control rats, as compared to only 13.3±0.1 and 13.7±0.4 fmol/min per cell in ω3D-NI and ω3-OO rats and 18.3±0.4 fmol/min per cell in ω3-FO rats. As expected from the time course for $^{86}Rb^+$ net uptake, these values were higher than those derived from the net uptake of ^{86}Rb after 10 min incubation. Expressed as fmol/cell per min, the latter values indeed only represented 70.5±2.3% (n=160) of the estimated inflow-outflow rate at isotopic equilibrium. In such a respect, there was no significant difference (p>0.3 or more) between the four groups of rats.

Taken as a whole, these findings indicate that the major defect of K^+ handling in ω3-depleted rats consists in a severe decrease in K^+ inflow into the cardiomyocytes. Such a decrease results in a parallel decrease of the equilibrium cell K^+ content. Both defects are antagonized, but not totally corrected, by the prior intravenous injection of the MCT:FO emulsion 60 min before sacrifice to the ω3-depleted animals.

^{45}Ca net uptake. Whether after 10 or 60 min incubation and whether in the presence of 5, 30 or 60 mM extracellular K^+, the net uptake of ^{45}Ca was significantly higher (p<0.001) in the ω3D-NI and ω3D-OO rats than in control animals, averaging respectively 134.0±3.3% (n=191) and 130.8±4.3% (n=171) in the ω3-NI and ω3D-OO rats of the mean corresponding values recorded under the same experimental conditions in control animals (100.0±3.0%; n=181). The mean percentages found in ω3D-NI and ω3D-OO rats failed to differ significantly (p>0.5) from one another. In the ω3D-FO rats, however, the mean percentage (99.1±2.9%; n=197) was significantly lower (p<0.001) than that recorded in the other ω3-depleted rats and, as a matter of fact, was virtually identical (p>0.8) to that found in the control animals (Table VII).

In all rats, the rise in extracellular K^+ concentration, which was osmotically compensated by an equimolar decrease in Na^+ concentration, resulted in an increased ^{45}Ca net uptake (Fig. 1). In the control rats and relative to the measurements made at 5 mM K^+, the values recorded after 10 and 60 min incubation averaged, respectively, 159.6±10.8% (n=26) and 130.3±3.2% (n=34) at 30 mM K^+ and 167.0±9.5% (n=28) and 157.4±4.2% (n=32) at 60 mM K^+. All these values were indeed significantly higher (p<0.001) than the corresponding measurements made in the same rats and at 5 mM K^+, i.e. 100.0±10.9% (n=27) after 10 min incubation and 100.0±3.5% (n=34) after 60 min incubation.

In the control rats and in all other animals, the mean net uptake of ^{45}Ca was lower at 30 mM than at 60 mM K^+, the results normalized relative to those found at 5 mM K^+ and recorded after 10 or 60 min incubation at 30 mM K^+ averaging 79.9±1.6% (n=244; p<0.001) of those recorded at the same time at 60 mM K^+ (100.0±1.5%; n=248).

Likewise, in the control rats and all ω3-depleted animals, the relative magnitude of the increase in ^{45}Ca net uptake caused by a rise in extracellular K^+ concentration was more marked after 10 min than after 60 min incubation, as expected from the fact that the depolarization of plasma membrane provoked by such a rise in K^+ concentration and the subsequent gating of voltage-sensitive Ca^{2+} affects the influx of the divalent cation into cells and, hence, is most obvious after 10 min incubation, i.e. at a time when the net uptake of ^{45}Ca depends mostly on the rate of Ca^{2+} inflow into the cardiomyocytes. As judged once again from the results normalized relative to those found at 5 mM K^+, those recorded at 30 and 60 mM K^+ averaged 226.5±5.0% (n=240) after 10 min incubation, as distinct (p<0.001) from only 132.2±2.4% (n=253) after 60 min incubation.

Table VIII. Na^+,K^+-ATPase activity in cardiomyocytes (pmol/ng DNA per 30 min).

Rats	Normal	ω3D-NI	ω3D-OO	ω3D-FO
Total	91.2±12.2 (5)	78.4±9.6 (5)	74.7±20.5 (5)	91.9±11.1 (5)
Ouabain-resistant	80.0±9.8 (5)	63.4±9.5 (5)	59.5±18.3 (5)	77.5±10.2 (5)
Ouabain-sensitive	11.3±2.4 (5)	15.1±1.7 (5)	16.1±2.5 (5)	14.3±1.3 (5)

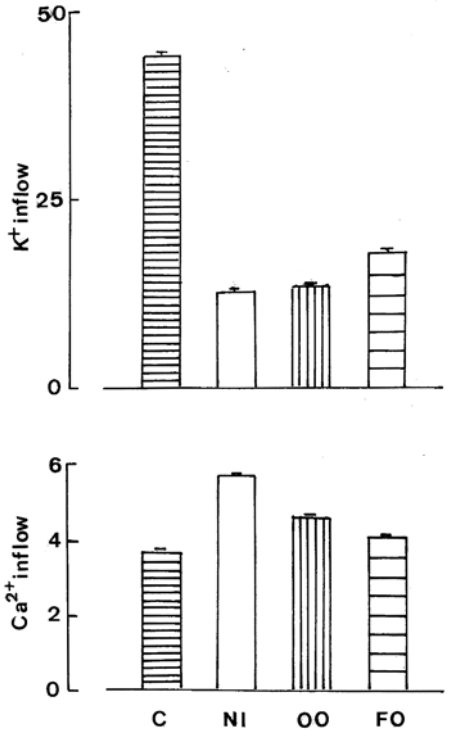

Figure 2. Basal K^+ inflow and Ca^{2+} inflow at 60 mM K^+ in cardiomyocytes from control (C), ω3D-NI (NI), ω3D-OO (OO) and ω3D-FO (FO) rats. Mean values (± deviation from mean value) are expressed as fmol/min per cell.

Relative to the net uptake of ^{45}Ca after 10 min incubation, that recorded after 60 min incubation was higher at normal extracellular K^+ concentration (5 mM) than at higher K^+ concentrations. Little difference was found between the 4 groups of rats when the islets were incubated at 60 mM K^+. Thus the 60 min values, expressed relative to the corresponding 10 min values, failed to differ significantly in control animals, ω3D-NI and ω3D-OO rats, and ω3-FO rats, with an overall mean value 178.9±2.3% (n=126) *versus* a reference value of 100.0±2.2% (n=122). At normal extracellular K^+ concentration (5 mM), however, the 60 min values progressively increased from 192.9±7.6% (n=34) in control rats to 230.0±7.9% (n=32) in ω3D-NI rats and 268.1±12.1% (n=33) in ω3D-FO rats. These findings imply that the fractional outflow rate of ^{45}Ca was lower in the ω3D-NI and ω3D-FO rats than in the control animals, when the cells were incubated at normal K^+ concentration. As shown in Table VII, such a fractional outflow rate indeed represented no more than 0.054 min^{-1} in the ω3D-NI rats and 0.042 min^{-1} in the ω3D-FO rats, as distinct form 0.072 min^{-1} in the control animals. At 60 mM K^+, however, the ^{45}Ca fractional outflow rate was comparable in these three groups of rats, with an overall mean value 0.083±0.002 min^{-1} (n=3).

At isotopic equilibrium, the estimated calcium content of cells exposed to 5 or 60 mM K^+ yielded ω3D-NI/control and ω3D-FO/control ratio of 142.0±2.6 and 109.7±3.6% (n=2 in both cases), respectively, and an ω3D-NI/ω3D-FO ratio of 129.5±1.8% (n=2). Such an equilibrium cell calcium content was thus significantly higher ($p<0.05$) in ω3D-NI rats than in either control of ω3D-FO rats, but not so in ω3D-FO *versus* control rats. The 60 mM/5 mM K^+ ratio for the equilibrium cell calcium content was virtually identical, however, in these three groups of rats, with an overall mean value 152.6±2.9% (n=3).

Last, as estimated from the equilibrium cell calcium content and ^{45}Ca fractional outflow rate, the rate of Ca^{2+} inflow and outflow, at isotopic equilibrium and at 5 mM K^+, was not significantly different ($p>0.1$ or more) in the control *versus* ω3D-NI or ω3D-FO rats, with an overall mean value of 1.96±0.19 fmol/min per cell (n=6). At 60 mM K^+, however, such a rate remained significantly higher ($p<0.01$ or less) in ω3D-NI rats (5.68±0.08 fmol/min per cell) and ω3D-FO rats (4.08±0.02 fmol/min per cell) than in control animals (3.70±0.02 fmol/min per cell).

In summary, as judged from the data computed at isotopic equilibrium, the depletion in ω3 fatty acids fails to affect Ca^{2+} inflow at 5 mM K^+, but enhances it at 60 mM K^+. Inversely, the calcium fractional outflow rate is decreased in the cardiomycotyes of ω3-depleted rats when exposed to 5 mM K^+, but unaffected at 60 mM K^+. As a result of these two situations, the equilibrium cell content is invariably higher in ω3D-NI rats than in control animals, whether at 5 or 60 mM K^+. The prior injection of the MCT:FO emulsion corrects the latter defect.

The internal consistency of this analysis is borne out by the data collected after 60 min incubation, i.e. close to isotopic equilibrium. Indeed, as illustrated in Fig. 1, at that time, the net uptake of ^{45}Ca averaged, in the ω3D-NI and ω3D-OO rats, 147.2±3.5% (n=181) of the corresponding mean values found at the same extracellular K^+ concentration in the control animals (100.0±3.3%; n=100), whilst the ω3D-FO rats yielded a mean value of 106.5±4.5%; n=99).

Likewise, there was a tight positive correlation (r=0.9961; n=6; $p<0.001$) between the estimated values for Ca^{2+} inflow-outflow at isotopic equilibrium, as listed in Table VII, and the corresponding values for the net uptake of ^{45}Ca after 10 min incubation, with a paired ratio between the latter uptake (expressed as fmol/min) and the former estimation of 69.7±1.7% (n=6), such a percentage being consistent with the exponential pattern for the time course of ^{45}Ca net uptake, progressively tending towards its equilibrium value.

results obtained in the ω3D-OO rats are not listed in, because no reliable data were obtained for the time course of ^{45}Ca net uptake at 5 mM K^+. However, at both 30 and 60 mM K^+, the results obtained in the ω3D-OO rats were essentially comparable to those collected in ω3D-NI rats (Fig. 1). For instance, at isotopic equilibrium, the estimated calcium content of the cardiomyocytes exposed to 30 and 60 mM K^+ averaged in the ω3D-OO rats 61.4±0.7 fmol/cell (n=4), as compared ($p>0.7$) to 60.2±3.0 fmol/cell (n=4) in the ω3D-NI rats.

Na^+,K^+-ATPase. The mean total ATPase activity and that resistant to ouabain were both lower in ω3D-NI rats than in control animals and in ω3D-OO rats than in ω3D-FO rats (Table VIII). Such a difference failed however to achieve statistical significance, the readings recorded in the ω3D-NI and ω3D-OO rats, expressed relative to the mean corresponding values found in control animals and ω3D-FO rats respectively (100.0±5.9%; n=20), averaging 80.8±8.3% (n=20; $p<0.08$). The absolute value for the ouabain-sensitive hydrolysis of ATP also failed to differ significantly ($p>0.15$) in the ω3D-NI and ω3D-OO rats (15.6±1.4 pmol/ng DNA; n=10) versus control and ω3D-FO rats (12.8±1.4 pmol/mg DNA; n=10). In the ω3D-NI and ω3D-OO it averaged 123.1±11.4% (n=10; $p>0.15$) of the mean corresponding values found in control animals and ω3D-OO rats, respectively (100.0±10.8%; n=10). As expected from these findings, the ouabain-sensitive hydrolysis of ATP represented a greater fraction ($p<0.01$) of the total ATPase activity in the ω3D-NI and ω3D-OO rats (21.6±2.1%; n=10) than in the control and ω3D-FO rats (14.3±1.1%; n=10).

Discussion

Second generation ω3-depleted rats represent a model for the decreased dietary intake of ω3 fatty acids often prevailing in Western populations. These rats display, in addition to several features of the metabolic syndrome (15-18) decreased basal cardiac function and impaired recovery following ischemia (5).

In the present study, the ventricular cardiomyocyte phospholipids of ω3-depleted rats were found to display severe depletion of all long-chain polyunsaturated ω3 fatty acids with a low C22:6ω3/C22:5ω3 ratio, increased amount of the three major long-chain polyunsaturated ω6 fatty acids (C18:2ω6, C20:4ω6 and C22:4ω6) with apparent facilitation of the generation of C20:4ω6 and C22:4ω6 from their respective precursors, elevated C16:1ω7/C16:0 and C18:1ω9/C18:0 ratios suggesting increased activity of Δ9-desaturase, and altered generation of the precursors of nervonic acid. All these features are comparable to those previously documented in both cardiac muscle and endothelium of second generation ω3-depleted rats (4,19).

These changes in the fatty acid pattern of phospholipids coincided with alteration of cationic fluxes in the ventricular cardiomyocytes prepared from ω3-depleted rats. Fig. 2 illustrates the two major anomalies in the handling of cations identified in ω3-depleted rats, namely the decrease in the basal rate of K^+ inflow and the increase in the rate of Ca^{2+} inflow observed a high extracellular K^+ concentration (60 mM). Fig. 2 also illustrates that both defects were partially corrected in cardiomyocytes from ω3-depleted rats injected intravenously 60 min before sacrifice with the MCT:FO emulsion. The results obtained in the latter rats were indeed closer to control values ($p<0.02$ or less) than those recorded in the ω3-depleted rats injected with the control ω3 fatty acid-poor MCT:OO emulsion.

The present findings concerning K^+ handling are reminiscent of those recently documented in rat pancreatic islets. Thus, in such islets, the net uptake of ^{86}Rb is also severely decreased in ω3-depleted rats. The impairment of K^+ inflow by an ouabain-sensitive modality, but no that mediated by an ouabain-resistant modality, is corrected by the prior intravenous administration of the MCT:FO, as distinct from MCT:OO, emulsion to the ω3-depleted rats (20).

Likewise, the islet calcium content at isotopic equilibrium is much higher in ω3D-OO rats than in control animals, whether at normal (5 mM) or higher (30 and 60 mM) extracellular K^+ concentrations. This islet defect is also partially corrected in the ω3D-FO rats (21).

The measurements of Na^+,K^+-ATPase activity in cardiomyocyte homogenates reinforce the view that the decrease of K^+ inflow found in intact cardiomyocytes from ω3-depleted rats is mainly attributable to alteration of an ouabain-resistant modality of K^+ entry into these cells. Indeed, in the cardiomyocyte homogenates, the ouabain-sensitive hydrolysis of ATP was not lower in ω3D-NI (ω3D-OO) rats than in control (or ω3D-FO) rats, and even represented a greater fraction of the total ATPase activity in the ω3D-NI and ω3D-OO rats than in the control and ω3D-FO rats.

In conclusion, the present results extend to intact ventricular cardiomyocytes the knowledge that, in ω3-depleted rats, the perturbation of the phospholipid fatty acid coincides with alteration of cationic fluxes and that the latter alteration may be, in part at least, corrected by the intravenous injection, 60 min before sacrifice, of an ω3-rich medium-chain triglyceride:fish oil emulsion.

Acknowledgments

We are grateful to A. Chwalik and A. Dufour for technical assistance and to C. Demesmaeker for secretarial help. This study was supported by Convention 5459 (Project WALNUT-20; Région Wallonne, Namur, Belgium).

References

1. Carpentier YA and Hacquebard M: Intravenous lipid emulsions to deliver omega 3 fatty acids. Prostaglandins Leukot Essent Fatty Acids 75: 145-148, 2006.
2. Portois L, Delckelbaum RJ, Malaisse WJ and Carpentier YA: Accumulation rapide d'eicosapentaenoate dans les phospholipides cellulaires après injection intraveineuse d'une émulsion d'huile de poisson et de triglycérides à chaîne moyenne à des sujets normaux. Nutr Clin Metabol 18 (Suppl 1): S53, 2004.
3. Pradier O, Portois L, Malaisse WJ and Carpentier YA: Hemostatic safety of the bolus intravenous injection of a novel medium-chain triglyceride:fish oil emulsion. Int J Mol Med 22: 301-307, 2008.
4. Portois L, Peltier S, Sener A, Malaisse WJ and Carpentier YA: Phospholipid and triglyceride fatty acid content and pattern in the heart of rats depleted in long-chain polyunsaturated ω3 fatty acids. Nutr Res 28: 51-57, 2008.

5. Peltier S, Malaisse WJ, Portois L, Demaison L, Novel-Chate V, Chardigny J-M, Sebedio JL, Carpentier YA and Leverve XM: Acute *in vivo* administration of a fish oil-containing emulsion improves post-ischemic cardiac function in ω3-depleted rats. Int J Mol Med 18: 741-749, 2006.
6. Courtois P, Louchami K, Portois L, Chardigny J-M, Sener A, Carpentier YA and Malaisse WJ: Effects of a medium-chain triglyceride:fish oil emulsion administered intravenously to ω3 fatty acid-depleted rats on cationic fluxes in aortic rings. Int J Mol Med 16: 1089-1093, 2005.
7. Fontaine D, Otto A, Portois L, Fontaine J, Berkenboom G, Malaisse WJ and Carpentier YA: Protection of aortic endothelial function in both normal and diabetic rats by intravenous bolus injection of a medium-chain triglyceride:fish oil emulsion. Int J Mol Med 18: 697-704, 2006.
8. Acar N, Chardigny J-M, Bonhomme B, Almanza S, Doly M and Sébédio JL: Long-term intake of trans (n-3) polyunsaturated fatty acids reduces the b-wave amplitude of electroretinograms in rats. J Nutr 132: 3151-3154, 2002.
9. Oguzhan B, Zhang Y, Louchami K, Courtois P, Portois L, Chardigny J-M, Malaisse WJ, Carpentier YA and Sener A: Pancreatic islet function in ω3 fatty acid-depleted rats. Glucose metabolism and nutrient-stimulated insulin release. Endocrine 18: 457-466, 2006.
10. Carpentier YA, Peltier S, Portois L, Sebedio JL, Leverve X and Malaisse WJ: Rapid reduction of liver steatosis in rats injected with a novel lipid emulsion. Horm Metab Res 40: 875-879, 2008.
11. Richelle M, Carpentier YA and Deckelbaum RJ: Long- and medium-chain triacylglycerols in neutral lipid-exchange processes with human plasma low-density proteins. Biochemistry 33: 4872-4878, 1994.
12. Simoens C, Richelle M, Rössle C, Derluyn M, Deckelbaum RJ and Carpentier YA: Manipulation of tissue fatty acid profile by intravenous lipids in dogs. Clin Nutr 14: 177-188, 1995.
13. Giroix MH, Agascioglu E, Oguzhan B, Louchami K, Zhang Y, Courtois P, Malaisse WJ and Sener A: Opposite effects of D-fructose on total versus cytosolic ATP/ADP ratio in pancreatic islet cells. Biochim Biophys Acta 1757: 773-780, 2006.
14. Malaisse WJ: Assessment of inflow rate, fractional outflow rate and steady-state cellular pool of ions based on two measurements of radioactive tracer net uptake. WSEAS Transactions Biol Med 3: 317-320, 2006.
15. Armitage JA, Pearce AD, Sinclair AJ, Vingrys AJ, Weisinger RS and Weisinger HS: Increased blood pressure later in life may be associated with perinatal n-3 fatty acid deficiency. Lipids 38: 459-464, 2003.
16. Cancelas J, Prieto PG, Villanueva-Peñacarrillo ML, Zhang Y, Portois L, Sener A, Carpentier YA, Valverde I and Malaisse WJ: Glucose intolerance associated to insulin resistance and increased insulin secretion in rats depleted in long-chain polyunsaturated ω3 fatty acids. Horm Metab Res 39: 823-825, 2007.
17. Carpentier YA, Peltier S, Portois L, Sener A and Malaisse WJ: Rapid lipid enrichment in ω3 fatty acids : plasma data. Int J Mol Med 21: 355-365, 2008.
18. Oguzhan B, Sancho V, Acitores A, Villanueva-Peñacarrillo ML, Portois L, Chardigny J-M, Sener A, Carpentier YA and Malaisse WJ: Alteration of adipocyte metabolism in ω3 fatty acid-depleted rats. Horm Metab Res 38: 789-798, 2006.
19. Carpentier YA, Portois L, Louchami K, Zhang Y, Sener A and Malaisse WJ: Phospholipid and triacylglycerol fatty acid content and pattern in the cardiac endothelium of rats depleted in long-chain polyunsaturated ω3 fatty acids. Cell Biochem Funct 26: 33-38, 2008.
20. Sener A, Zhang Y, Louchami K, Oguzhan B, Courtois P, Portois L, Chardigny J-M, Carpentier YA and Malaisse WJ: Alteration of K^+ fluxes and insulin release in pancreatic islets from ω3 fatty acid-depleted rats. Endocrine 30: 207-211, 2006.
21. Zhang Y, Oguzhan B, Louchami K, Chardigny J-M, Portois L, Carpentier YA, Malaisse WJ, Herchuelz A and Sener A: Pancreatic islet function in ω3 fatty acid-depleted rats: alteration of calcium fluxes and calcium-dependent insulin release. Am J Physiol 291: E441-E448, 2006.